7ICMSNSE-32

Preliminary Performance Evaluation of On-the-Fly Doppler Broadening Capability for Monte Carlo Simulation in MCS

A. Khassenov, S. Choi, H. Lee, P. Zhang, Y. Zheng and D. Lee

Ulsan National Institute of Science and Technology, 50, UNIST-gil, Ulsan, Republic of Korea <u>azamat@unist.ac.kr</u>, <u>csy0321@unist.ac.kr</u>, <u>huynsuklee@unist.ac.kr</u>, <u>zhangpeng@unist.ac.kr</u>, <u>yqz</u> <u>heng@unist.ac.kr</u>, <u>deokjung@unist.ac.kr</u>

Abstract

This paper examines multipole representation of the cross section and its further Doppler broadening at the resolved resonance region. At the first step, a conversion is performed from nuclear data file resonance parameters to multipoles, which are corresponding poles and residues. The application of multipole representation allows generating the cross section at the target temperature, without pre-generation of 0K cross section libraries. In order to reduce the computational time for cross section generation, window energy concept was implemented and tested. On-the-fly Doppler broadening module based on multipole and windowed multipole representations were implemented into Monte Carlo code, and a pin cell problem was simulated. Simulation time and multiplication factors for different cases were compared with original Monte Carlo simulation results.

Keywords: Breit-Wigner formalism, Reich Moore, Multipole representation, Poles and Residues, Level matrix

1. Introduction

Monte Carlo Simulation allows the design and analysis of different nuclear reactors in terms of neutron physics. By coupling neutron physics and thermo-hydraulics codes, it is possible to obtain thermo-hydraulic feedback, which currently requires pre-generated cross section data at 10-50 K intervals. On-the-Fly Doppler broadening is a technique to avoid pre-generation of the microscopic cross section, in other words, to reduce the amount of storage. Currently, there are different types of formalisms used by the NJOY code to generate reaction cross sections and accomplish its Doppler broadening [1]. Single-Level Breit-Wigner (SLBW) formalism is limited to well-separated resonances; in other words, it does not consider interference between energy levels. Multi-Level Breit-Wigner formalism (MLBW) was tested as the candidate for the cross section generation in the Monte Carlo code, which is under development at UNIST. This Monte Carlo code named "MCS" has 3D whole core modelling capability [2]. According to the results, the MLBW method requires a huge amount of computational time to produce cross sections at certain energy points [3]. The Reich-Moore (RM) technique can generate only 0K cross sections, which means that it cannot produce broaden cross section directly from resonance parameters. Adler-Adler formalism is used only

for s-wave resonances, but most nuclides of great interest have higher angular momentum states.

In this paper, Multipole representation (MPR), proposed by Hwang [4], is used as the cross section generation formalism, which allows application of Doppler broadening using the Faddeeva function. This method requires conversion of resonance parameters from nuclear data files to corresponding multipoles, which are poles and residues. Implementation of the energy window concept reduce the overall computational time required for cross section generation [5].

2. Multipole representation

Multipole representation is an alternative to the conventional R-Matrix theory to describe the microscopic cross sections of different nuclides in the resolved resonance region. It is the general form of the rationalization suggested by Saussure and Perez, which was limited only to s-wave resonances. Hwang extended this concept for higher angular momentums. This formalism is based on the physical condition that the collision matrix is single valued and meromorphic in the momentum space. Eqs. (1), (2), and (3) show radiative capture and fission, total, and elastic scattering reaction microscopic cross sections, respectively, in terms of multipole resonance parameters.

$$\sigma_{x=\gamma,f} = \frac{1}{E} \sum_{l,J} \sum_{\lambda}^{N} \sum_{j=1}^{2(l+1)} \operatorname{Re} \left[\frac{\left(-iR_{l,J,\lambda,j}^{(x)}\right)}{p_{l,J,\lambda,j}^* - \sqrt{E}} \right]$$
(1)

$$\sigma_{t} = \frac{1}{E} \sum_{l,J} \sum_{\lambda}^{N} \sum_{j=1}^{2(l+1)} \text{Re} \left[\frac{\left(-ie^{-i2\phi_{l}} R_{l,J,\lambda,j}^{(t)} \right)}{p_{l,J,\lambda,j}^{*} - \sqrt{E}} \right]$$
 (2)

$$\sigma_{s} = \sigma_{t} - \sigma_{f} - \sigma_{v} \tag{3}$$

where l, J are relative orbital angular momentum and total spin; λ, N are resonance index and total number of resonances; $R_{l,J,\lambda,j}^{(x)}, p_{l,J,\lambda,j}^*, E$ are residue corresponding to the reaction x, complex conjugate of the resonance pole, and energy, respectively.

2.1 Conversion of parameters

The first step to perform multipole representation is generation of poles and residues using resonance parameters, which are given in the nuclear data files [6]. In addition, the energy domain should be converted to the momentum domain, where the physical condition is satisfied. Currently, in order to construct the resolved resonance region cross section there are two main formalisms used: MLBW and RM. Therefore, for each of these methods there are different formats of the given resonance parameters in the nuclear data file. Conversion of

parameters for MLBW and RM is different, since different assumptions are made for each method.

In the case of the Single- and Multi-Level Breit-Wigner formalisms, the R matrix is represented in terms of the level matrix $A_{\lambda}^{(l)}$ approximations. As was mentioned, SLBW can be applied only to well-separated resonances, because the level matrix is assumed to consist of the single element. In contrast, in the MLBW technique the level matrix is assumed to be a diagonal matrix, which allows consideration of interference between the energy levels of the given (l,J)-state. Hence, there is an interference microscopic cross section term, which is shown in Eqs. (4) and (5).

$$\sigma_t^{MLBW} = \sigma_t^{SLBW} + \sigma_{\text{int}} \tag{4}$$

$$\sigma_{\text{int}} = \sum_{l,J} \frac{\pi}{k^2} g_J \operatorname{Re} \left\{ \sum_{\lambda}^{N} \sum_{\substack{\mu=1\\\mu \neq \lambda}}^{N} \frac{\Gamma_{\lambda n}^{(l)}(u) \Gamma_{\mu n}^{(l)}(u)}{A_{\lambda}(u) A_{\mu}^{*}(u)} \right\}$$
(5)

where $k = k_0 \sqrt{E} = 2.196771 \times 10^3 \times \frac{A}{A+1} \times \sqrt{E}$ is the wave number in the center-of-mass system; A is the ratio of the particular isotope's mass to that of a neutron; $u = \sqrt{E}$; g_J is the statistical spin factor; $\Gamma_{\lambda n}^{(l)}(u) = \Gamma_{\lambda n} \frac{P_0(u)}{P_0(|E_{\lambda}|)}$ is the neutron width, and $\Gamma_{\lambda n}$ is the neutron width at resonance energy.

In order to find out the resonance poles, it is necessary to solve the polynomial given in Eq. (6).

$$q_{l}(u)A_{\lambda}^{(l)}(u) = \sum_{m=0}^{2(l+1)} a_{\lambda,m}^{(l)} u^{m} = 0$$
(6)

where $a_{\lambda,m}^{(l)}$ is a polynomial coefficient and $q_l(u)$ is a function defined in Table I.

Table I: The l- dependent Functions

Angular momentum	S_l	q_l	ϕ_l
0	0	1	ρ
1	1	$1 + \rho^2$	$ ho$ – $ an^{-1}(ho)$
2	$18+3\rho^2$	$9+3\rho^2+\rho^4$	$\rho - \tan^{-1} \left(\frac{3\rho}{3 - \rho^2} \right)$

Eqs. (7) and (8) show the level matrix and level shift, respectively.

$$A_{\lambda}^{(l)}(u) = \left[E_{\lambda} + \Delta_{\lambda}^{l}(u) - (u)^{2}\right] - \frac{i}{2}\left[\Gamma_{\lambda n}^{(l)}(u) + \Gamma_{\lambda \gamma} + \Gamma_{\lambda f}\right]$$

$$\tag{7}$$

$$\Delta_{\lambda}^{l}(u) = \Gamma_{\lambda n} \frac{S_{l}(|E_{\lambda}|) - S_{l}(|u|)}{2P_{l}(|u|)}$$
(8)

where E_{λ} , $\Gamma_{\lambda\gamma}$, $\Gamma_{\lambda f}$ are resonance energy, capture width, and fission width; $S_{l}(u)$, $P_{l}(u)$ are shift and penetration factors, respectively, which are shown in Table II.

It can be seen from Eq. (6) that in the case of orbital angular momentum l there is a polynomial of order 2(l+1).

$$\rho = \rho_0 \times u = (k_0 a) \times u = \left(2.196771 \times 10^3 \times \frac{A}{A+1} \times a\right) \times u \tag{9}$$

where a is the interaction radius (channel radius).

Table II: Shift and Penetration Factors

Angular momentum	Shift Factor	Penetration Factor
0	0	ρ
1	$-\frac{1}{1+\rho^2}$	$\frac{\rho^3}{1+\rho^2}$
2	$-\frac{18+3\rho^2}{9+3\rho^2+\rho^4}$	$\frac{\rho^5}{9+3\rho^2+\rho^4}$

By using Eq. (6) and the definition of the level matrix with respect to the formalism type it is possible to find out the coefficients of the polynomial. In this study, a polynomial solver based on Laguerre's method was used in order to calculate poles. Table III shows poles of the swave resonance at energy 2810 eV for Na²³:

Table III: Na²³ poles for l = 0, J = 1 (ENDF/B-VII.1)

Energy (eV)	$\operatorname{Re}ig(p^*ig)$	$\operatorname{Im}\!\left(p^* ight)$
2.810E+03	5.2979765E+01	1.7749350E+00
2.810E+03	-5.2979765E+01	1.7716036E+00

After finding the poles, it is possible to calculate residues with respect to every cross section type such as total, capture, fission, and interference. Eqs. (10), (11), and (12) show the derived reaction residues.

$$R_{l,J,\lambda,j}^{(t)} = \frac{2\pi}{k_0^2} g_J \times \frac{q_l \left(p_{l,J,\lambda,j}^* \right) \times \Gamma_{\lambda n}^{(l)} \left(p_{l,J,\lambda,j}^* \right)}{-\rho_0^{2l} \prod_{\substack{k=1\\k \neq i}}^{2(l+1)} \left(p_{l,J,\lambda,j}^* - p_{l,J,\lambda,k}^* \right)}$$
(10)

$$R_{l,J,\lambda,j}^{(x=\gamma,f)} = R_{l,J,\lambda,j}^{(t)} \times \frac{\Gamma_{\lambda n}}{\Gamma_{\lambda n}^{(l)} \left(p_{l,J,\lambda,j}^*\right) + \Gamma_{\gamma n} + \Gamma_{fn}}$$

$$\tag{11}$$

$$R_{l,J,\lambda,j}^{(\text{int})} = R_{l,J,\lambda,j}^{(t)} \times i \left[\sum_{\substack{\mu=1\\\mu \neq \lambda}}^{N} \frac{\Gamma_{\mu m}^{(l)} \left(p_{l,J,\lambda,j}^{*} \right)}{A_{\mu}^{r} \left(p_{l,J,\lambda,j}^{*} \right) + i A_{\mu}^{i} \left(p_{l,J,\lambda,j}^{*} \right)} \right]$$
(12)

2.2 Doppler broadening

There are different ways of performing Doppler broadening. In the case of most nuclides of the great interest, the NJOY code pre-generates the 0K cross section using the RECONR module, which further is broadened by a different module, called BROADR.

On the other hand, MPR allows production of the cross section at certain temperatures directly from resonance poles and residues, which are generated as shown in the previous section. Doppler-Broadened line-shape functions $\psi - \chi$ are used to modify the cross section with respect to the temperature, while MPR is generating it [7]. It is based on the Faddeeva function as shown in Eq. (13).

$$W(z) = \frac{i}{\pi} \int_{-\infty}^{\infty} \frac{e^{-t^2} dt}{z - t} = \frac{2}{\sqrt{\pi \theta}} (\psi(x, \theta) + i\chi(x, \theta))$$
(13)

where $z = x + i\theta$ is the complex variable.

The reaction microscopic cross sections given in Eqs. (1), (2), and (3) transform into the temperature dependence forms given in Eqs. (14) and (15).

$$\sigma_{x=\gamma,f} = \frac{1}{E} \sum_{l,J} \sum_{\lambda}^{N} \sum_{j=1}^{2(l+1)} \frac{\text{Re} \left[R_{l,J,\lambda,j}^{(x)} \sqrt{\pi} W(z_0) - \frac{-i R_{l,J,\lambda,j}^{(x)}}{\sqrt{\pi}} C\left(\frac{p_{l,J,\lambda,j}^*}{\sqrt{\xi}}, \frac{\sqrt{E}}{2\sqrt{\xi}}\right) \right]}{2\sqrt{\xi}}$$
(14)

$$\sigma_{t} = \sigma_{p}\left(E\right) + \frac{1}{E} \sum_{l,J} \sum_{\lambda} \sum_{j=1}^{N} \sum_{j=1}^{2(l+1)} \frac{\operatorname{Re}\left[R_{l,J,\lambda,j}^{(t)} \sqrt{\pi}W\left(z_{0}\right) - \frac{-iR_{l,J,\lambda,j}^{(t)}}{\sqrt{\pi}}C\left(\frac{p_{l,J,\lambda,j}^{*}}{\sqrt{\xi}}, \frac{\sqrt{E}}{2\sqrt{\xi}}\right)\right]}{2\sqrt{\xi}}$$

$$(15)$$

where
$$z_0 = \frac{\sqrt{E} - p_{l,J,\lambda,j}^*}{2\sqrt{\xi}}$$
; $\xi = \frac{k_b T}{4A}$; k_b is the Boltzmann's constant; and T is target temp

erature. Hwang noticed that correction factor $C\left(\frac{p_{l,J,\lambda,j}^*}{\sqrt{\xi}}, \frac{\sqrt{E}}{2\sqrt{\xi}}\right)$ is only significant at ve ry low energies, and it can be neglected at higher energies [8].

2.3 Energy Window Concept

The total number of multipoles required for processing U²³⁸ is 3364. According to the conventional Doppler broadening, all existing multipoles of the given isotope should be used to generate the cross section for the target temperature at every single energy point. In recent study, however, it was noticed that temperature dependence of the cross section at the given energy point is effected by the neighbouring resonances [9].

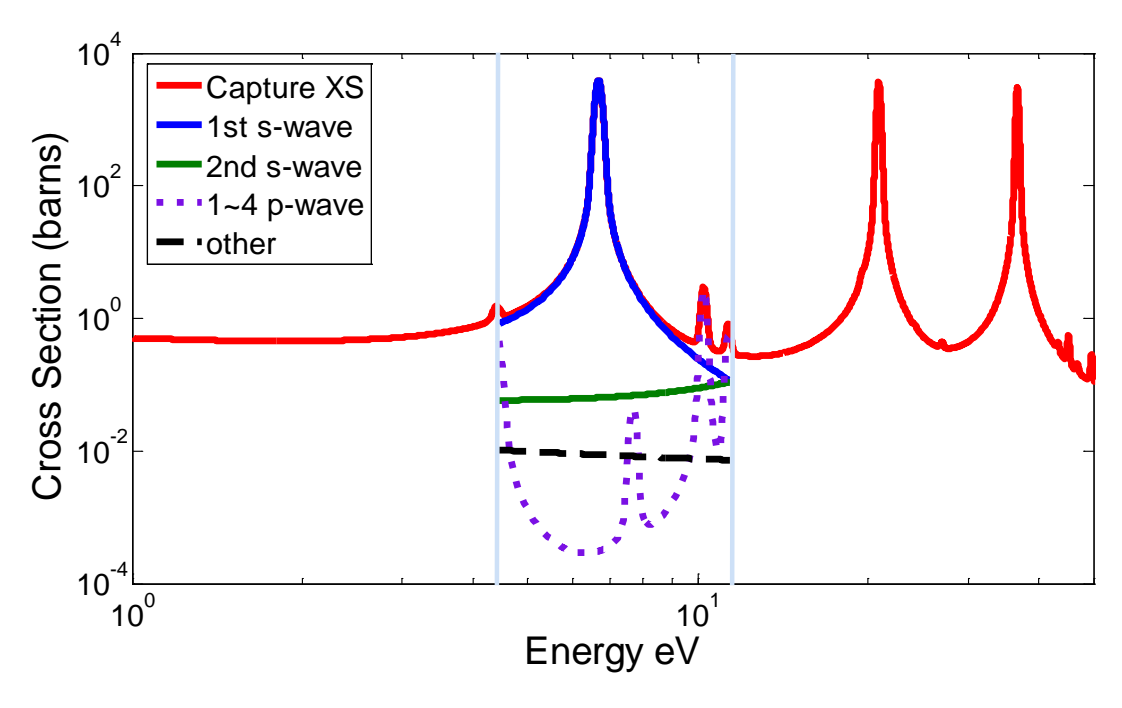


Figure 1 Energy window for capture cross section of the U²³⁸.

Fig. 1 shows the basic concept of the energy window method. Only resonances within this window are broadened and the remaining resonances outside the given energy region stays at 0 K. In other words, the cross section at the specific temperature is the summation of broaden and 0 K resonances. The 0 K cross section does not require the evaluation of the Faddeeva function. Instead of the computing the Faddeeva function, Voigt profiles at 0 K are used as shown in Eqs. (16), (17) and (18).

$$\psi(x,0) = \frac{1}{1+x^2} \tag{16}$$

$$\chi(x,0) = \frac{x}{1+x^2} \tag{17}$$

$$x = \frac{\sqrt{E} - \text{Re}\left(p_{l,J,\lambda,j}^*\right)}{\text{Im}\left(p_{l,J,\lambda,j}^*\right)}$$
(18)

This approach requires less computation resources than evaluation of the Faddeeva function. Therefore, energy window method causes the decrease in the overall computational time required for cross section generation.

3. Results

After implementation of the on-the-fly Doppler broadening module into MCS for the resolved resonance region (RRR), a Mosteller benchmark MOX pin cell problem was simulated, which has PuO₂ of 1.0 wt. % at hot zero power (HZP) conditions [10]. All simulations used 50 inactive, 1000 active cycles, and 10,000 neutron histories per cycle. The given problems were computed using 40 cores of a parallel Linux cluster. The description of energy bins used for tally of the neutron flux is given in Table IV.

Bin Index	Bottom of Bin (eV)	Top of Bin (eV)	Bin Index	Bottom of Bin (eV)	Top of Bin (eV)
1	3.00E-02	1.00E-01	8	1.00E+01	2.50E+01
2	1.00E-01	3.00E-01	9	2.50E+01	5.00E+01
3	3.00E-01	6.25E-01	10	5.00E+01	1.00E+02
4	6.25E-01	1.00E+00	11	1.00E+02	1.00E+03
5	1.00E+00	4.00E+00	12	1.00E+03	1.00E+04
6	4.00E+00	6.00E+00	13	1.00E+04	1.00E+05
7	6.00E+00	1.00E+01			

Table IV: Energy tally bins

In order to perform the on-the-fly Doppler broadening with multipole representation, the nuclear data in MC2-3 library were used, in which the ENDF Reich Moore resonance parameters were already converted to the multipoles [11]. In this preliminary tests, the on-the-fly Doppler broadening module was applied only for three isotopes, U²³⁵, U²³⁸, and Pu²⁴¹ within corresponding energy regions from 1.2 eV up to 2.2 keV, from 4.4 eV up to 20 keV, and from 1.7 eV up to 300 eV, respectively. In Figs. 2 to 3, the tallied flux spectra and absolute relative differences are shown for those 3 isotopes with multipole and windowed multipole.

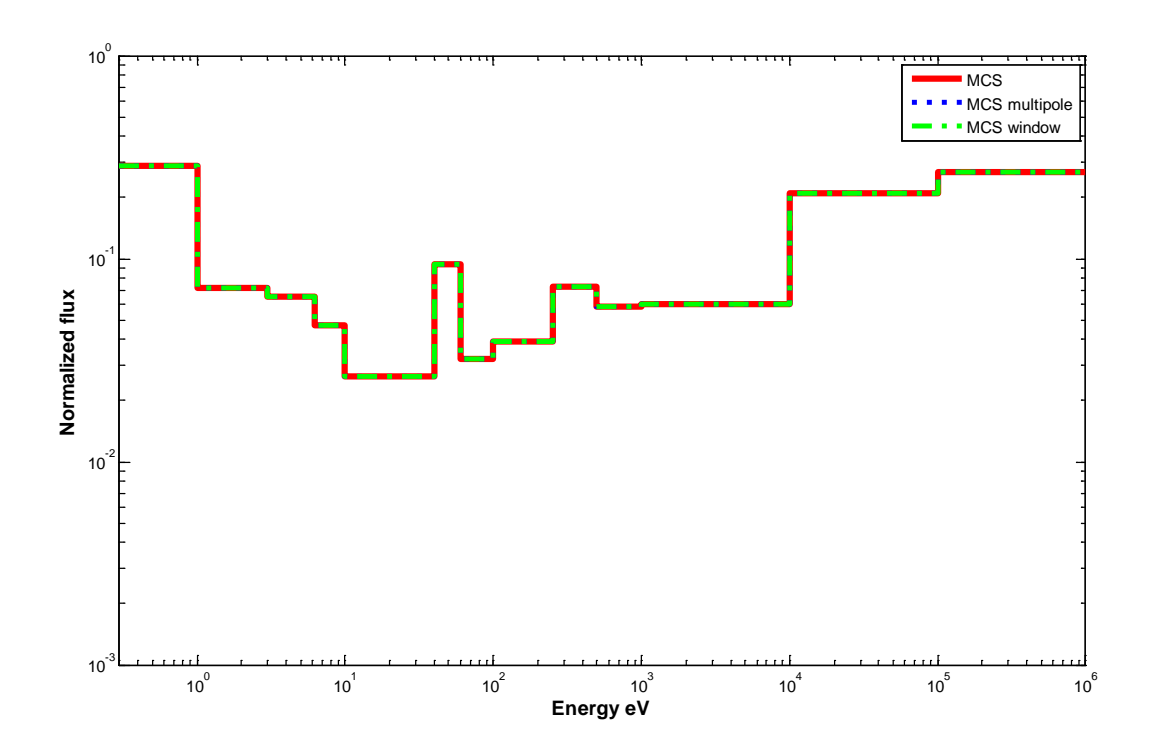


Figure 2 Comparison of fuel region energy spectra for MCS with ACE cross sections, MCS with multipole, and MCS with windowed multipole.

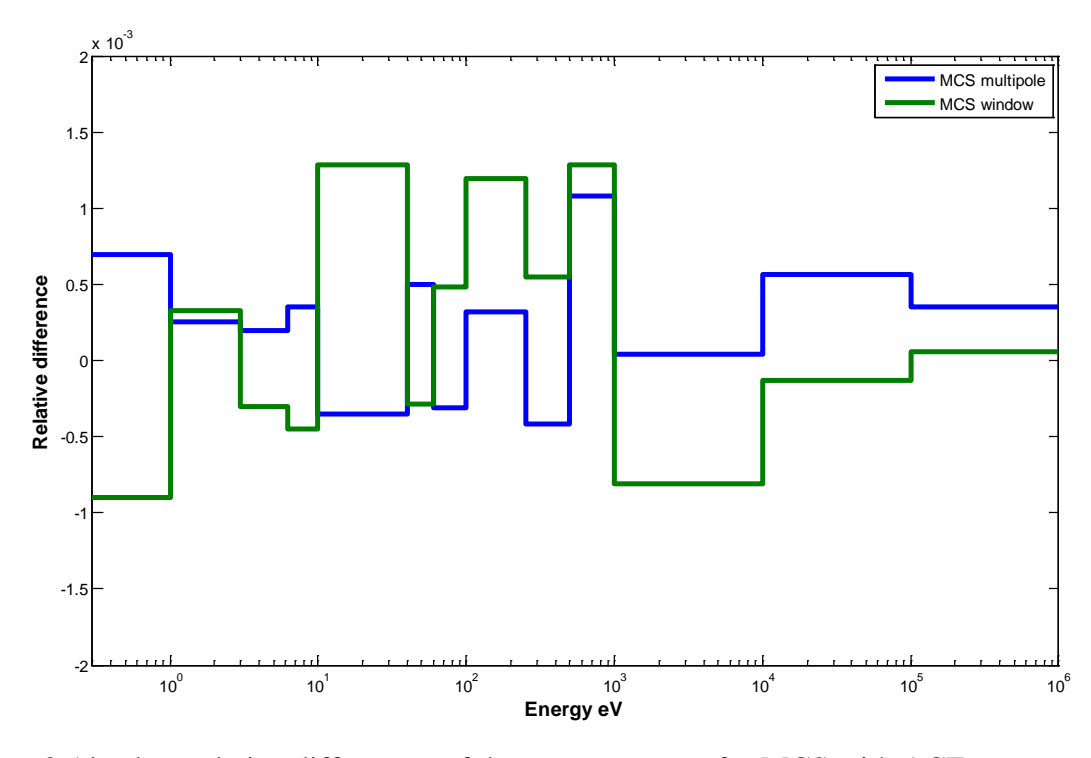


Figure 3 Absolute relative differences of the energy spectra for MCS with ACE cross sections, MCS with multipole, and MCS with windowed multipole.

Figs. 2 and 3 present the neutron spectrum and the absolute relative difference for the corresponding energy bins. According to the neutron spectrum comparison, absolute relative difference is less than 0.15% for all energy bins. Table V shows the simulation results for the separate isotopes, and 3 isotopes simultaneously applied into multipole and windowed multipole method. In addition, the time ratios are provided with respect to the MCS original, which uses only ACE format cross section. There are 3193, 3343, and 244 resolved resonances for U²³⁵, U²³⁸, and Pu²⁴¹, respectively. According to the results given in table below, it is noticed that the difference in the number of resonances causes difference in the time ratio.

	Isotope	k-eff (STD)	Difference (pcm)	Time Ratio
MCS	-	0.95928 (0.00020)	-	1
MCS multipole	U^{235}	0.95956 (0.00020)	-28	6.90
MCS windowed multipole	U ²³⁵	0.95952 (0.00020)	-24	4.11
MCS multipole	U^{238}	0.95942 (0.00020)	-14	8.75
MCS windowed multipole	U^{238}	0.95947 (0.00020)	-19	6.77
MCS multipole	Pu ²⁴¹	0.95972 (0.00020)	-44	1.75
MCS windowed multipole	Pu ²⁴¹	0.95897 (0.00020)	31	1.19
MCS multipole	U^{235} , U^{238} , Pu^{241}	0.95912 (0.00020)	16	25.93
MCS windowed multipole	$U^{235}, U^{238}, Pu^{241}$	0.95958 (0.00019)	-30	10.67

Table V: Multiplication Factor Comparison

4. Conclusion

Multipole representation and Doppler-broadened line shape functions were used to construct the microscopic cross section of U²³⁵, U²³⁸ and Pu²⁴¹ at different temperatures. Mosteller benchmark MOX fuel pin cell problem was tested for the verification of the on-the-fly Doppler broadening based on multipole and windowed multipole representations. The window concept was applied for each isotope and preliminary window ranges were determined. However, more studies about window size sensitivity need to be done. According to the results given in Table V the windowed multipole representation shows very high potential to be used as the formalism in the on-the-fly Doppler broadening module of MCS.

Further improvements in terms of computational time and cross section accuracy can be achieved through more detailed studies of the conversion of resonance parameters and energy window size sensitivity. Additionally, the overall algorithm of the on-the-fly Doppler broadening module need to be optimized.

5. Acknowledgements

This work was supported by a National Research Foundation of Korea (NRF) grant funded by the Korean government (MSIP).

Authors thank Prof. Ben Forget and his students Pablo Ducru and Coley Josey for assistance with understanding the multipole representation and conversion of resonance parameters into multipoles.

6. References

- [1] R. E. MacFarlane, D. W. Muir, R. M Boicourt, A. C. Kahler, The NJOY Nuclear Data Processing System, Version 2012, 2012.
- [2] H. Lee, C. Kong, and D. Lee, "Status of Monte Carlo Code Development at UNIST," PHYSOR 2014, Kyoto, Japan, 2014.
- [3] A. Khassenov, S. Choi, and D. Lee, "Application of Energy Window Concept in Doppler Broadening of 238U Cross Section," Transactions of KNS-2014, Pyeongchang, Korea, 2014.
- [4] R. N. Hwang, "A Rigorous Pole Representation of Multilevel Cross Sections and Its Practical Applications," *Nuclear Science and Engineering*, Vol. 96, pp. 129-209, 1987.
- [5] B. Forget, S. Xu, and K. Smith, "Direct Doppler broadening in Monte Carlo simulations using the multipole representation," *Annals of Nuclear Energy*, Vol. 64, pp. 78-85, 2014
- [6] C. Jammes and R. N. Hwang, "Conversion of Single- and Multilevel Breit-Wigner Resonance Parameters to Pole Representation Parameters," *Nuclear Science and Engineering*, Vol. 134, pp. 37-49, 2000.
- [7] Y. Azmy and E. Sartori, "Resonance Theory in Reactor Applications," Nuclear Computational Science: A Century in Review, pp. 217-290, 2010.
- [8] R. N. Hwang, "An Extension of the Rigorous pole representation of cross sections for reactor applications," *Nuclear Science and Engineering*, Vol. 111, pp. 113-131, 1992.
- [9] C. Josey, P. Ducru, B. Forget, and K. Smith, "Windowed Multipole for Cross Section Doppler Broadening," *Journal of Computational Physics*, doi:10.1016/j.jcp.2015.08.013, 2015
- [10] R. D. Mosteller, "The Doppler-effect Benchmark: Overview and Summary of Results," *M&C* 2007, Monterey, California, USA. 2007

- [11] C. H. Lee and W. S. Yang, "MC2-3: Multigroup Cross Section Generation Code for Fast Reactor Analysis," 2013.
- [12] C. Josey, B. Forget, and K. Smith, "Efficiency and Accuracy of the Windowed Multipole Direct Doppler Broadening Method," *PHYSOR 2014*, Kyoto, Japan, 2014.